A&A 394, 107–113 (2002)
DOI: 10.1051/0004-6361:20021097

Astronomy & Astrophysics

Discovery of new highly excited OH sources in regions of high-mass star formation

A. Baudry[1] and J. F. Desmurs[1,2]

[1] Observatoire de l'Université de Bordeaux 1, BP 89, 33270 Floirac, France
[2] Observatorio Astronómico Nacional, Apartado 1143, 28800 Alcalá de Henares, Spain

Received 20 March 2002 / Accepted 29 July 2002

Abstract. We have carried out sensitive observations of the highly excited $^2\Pi_{\frac{3}{2}}, J = \frac{7}{2}$ state of OH (290 K above the ground-level) at 13 441 MHz ($F = 4 - 4$) and 13 435 MHz ($F = 3 - 3$) in both right and left circular polarizations with the Effelsberg 100-m telescope. Our sample included 27 compact or ultra-compact HII regions. Most of them have been selected from our previous $J = \frac{5}{2}$ OH maser survey of star-forming regions taken from the IRAS point-source catalog. We have observed weak $^2\Pi_{\frac{3}{2}}, J = \frac{7}{2}, F = 4 - 4$ and $3 - 3$ absorption in 7 sources and discovered 3 new weak $F = 4 - 4$ maser sources at 13 441 MHz in addition to W3(OH). The new sources, 20081+3122 (ON1), 21413+5442 and G11.90−0.14, are 50 to 100 times or more weaker than the 13 441 MHz peak flux density observed in W3(OH). 21413+5442 and G11.90−0.14 exhibit extremely narrow velocity extents of the order of 0.4 km s^{-1}. However, in ON1 there are two groups of narrow velocity features separated by about 14 km s^{-1}; these two groups are also observed in lower rotational levels and suggest complex kinematics in the envelope of the young ultra-compact HII region.
Apart from a very weak, polarized, and narrow $J = \frac{7}{2}, F = 3 - 3$ emission feature lying on the red wing of the 13 435 MHz absorption feature in W3(OH) no $J = \frac{7}{2}, F = 3 - 3$ emission was discovered.
We conclude that the 13 441 MHz OH maser emission from W3(OH) remains exceptionally strong but not unique. In contrast with the $J = \frac{5}{2}$, 6035 MHz maser emission observed in a large number of star-forming regions, $J = \frac{7}{2}$, 13 441 MHz emission is not widespread. This is expected from OH maser theory, and because the involved $J = \frac{7}{2}$ levels are high in the OH energy ladder and not directly connected to the ground-state.

Key words. ISM: HII regions – ISM: molecules – masers – stars: formation

1. Introduction

Maser emission from both the ground- and excited-states of OH allows us to trace kinematical and physical properties of the neutral gas lying in the immediate vicinity of compact HII regions associated with embedded high mass stars. In addition, the excited-states of OH help us to understand the various pumping routes leading to the OH maser phenomenon. Among all of the excited-state transitions of OH that have been detected in space, the $^2\Pi_{\frac{3}{2}}, J = \frac{7}{2}, F = 4 - 4$ transition observed at 13 441 MHz seems unique because: (*a*) $F = 4 - 4$ maser emission has been detected in only one source W3(OH), and (*b*) this hyperfine transition is a strong maser although it is the most highly excited transition known to date (the $J = \frac{7}{2}$ state is 290 K above the ground-level).

Sensitive, single dish observations of the $J = \frac{7}{2}$ OH level were first performed in W3(OH) with the 100-m telescope (Baudry et al. 1981; Güsten et al. 1994). Strong $F = 4 - 4$ emission and $F = 3 - 3$ absorption are simultaneously present and may be used to estimate the magnetic field strength (Güsten et al. 1994). Baudry & Diamond (1998) used the VLBA to make polarization images of the $F = 4 - 4$ maser emission and to identify several Zeeman pairs in the OH gas. Beyond the extensive work available in W3(OH) it now seems useful to extend the search for $J = \frac{7}{2}$ OH emission or absorption to selected HII regions. Theory of OH masers predicts, in agreement with observations, that OH tends to be more easily excited in the lower J levels. However, theory does not predict any sharp cut-off of OH emission at any particular J level and sensitive observations should result in the discovery of new $J = \frac{7}{2}$ sources and should tell us whether this state and W3(OH) are truly unique or not.

In Sect. 2 we present our source sample, the observations and our results. The emission and absorption results are discussed in Sect. 3.

Send offprint requests to: A. Baudry,
e-mail: baudry@observ.u-bordeaux.fr

2. Observations and results

2.1. Source sample and observations

The large number of 6035 MHz $J = \frac{5}{2}$ OH maser sources detected toward compact HII regions of the Northern and

Table 1. Observations of the 13 435 and 13 441 MHz transitions of OH.

IRAS Source	Other Name	Observed Coordinates J2000.0		LSR Velocity	Sensitivity[a] (Jy)			
		RA	Dec	Range (km s^{-1})	13 435 MHz		13 441 MHz	
		h m s	° ′ ″		RCP	LCP	RCP	LCP
02232+6138	W3(OH)	02:27:03.88	+61:52:24.57	−210, +850	*A*	*E*, *A*	*E*, *A*	*E*, *A*
	G0.66−0.03	17:47:19.00	−28:22:52.36	−150, +290	< .33	< .33	< .33	< .33
	G11.90−0.14	18:12:11.56	−18:41:29.61	−177, +263	< .17	< .17	*E*	< .17
	W33B	18:13:55.51	−18:01:50.51	−185, +260	< .21	< .21	< .21	< .21
	W33C	18:14:13.67	−17:55:25.18	−185, +335	*A*?	*A*?	*A*	*A*
18117−1753	W33A	18:14:39.50	−17:52:00.30	−185, +250	< .21	< .21	< .21	< .21
	G20.23+0.07	18:27:44.10	−11:14:54.02	−148, +292	< .15	< .15	< .15	< .15
18174−1612	M 17	18:20:22.43	−16:11:25.29	−200, +240	< .20	< .20	< .20	< .20
18403−0417	OH28.21	18:42:58.18	−04:13:59.84	−120, +320	< .19	< .19	< .19	< .19
18507+0110	OH34.26	18:53:19.40	+01:14:34.72	−150, +290	< .18	< .18	< .18	< .18
18515+0157*	OH35.03	18:54:04.21	+02:01:33.93	+27, +62	< .13	< .13	< .13	< .13
18592+0108	W48	19:01:46.96	+01:13:07.60	−178, +272	< .24	< .24	< .24	< .24
19078+0901	W49	19:10:15.31	+09:06:08.48	−225, +215	*A*?	*A*?	*A*	*A*
19111+1048	OH45.12	19:13:27.81	+10:53:33.92	−162, +278	*A*	*A*	*A*	*A*
19120+1103*		19:14:21.73	+11:09:13.66	+22, +92	< .10	< .10	< .10	< .10
19201+1400		19:22:26.59	+14:06:36.12	−150, +290	< .16	< .16	< .16	< .16
19213+1424	W51	19:23:39.95	+14:30:51.14	−164, +276	*A*?	*A*?	*A*	*A*
19598+3324	K3-50	20:01:45.59	+33:32:44.12	−240, +200	*A*	*A*	*A*	*A*
	ON3	20:01:53.98	+33:34:13.64	−235, +205	< .21	< .21	< .21	< .21
20081+3122	ON1	20:10:09.14	+31:31:34.37	−215, +225	< .15	< .15	*E*	*E*
20350+4126	DR20	20:36:52.61	+41:36:32.59	−276, +164	< .18	< .18	< .18	< .18
	W75N	20:38:36.93	+42:37:37.52	−213, +227	< .15	< .15	< .15	< .15
(*)	DR21(OH)	20:39:00.60	+42:22:48.84	−40, +30	< .10	< .10	< .10	< .10
	W75S(3)	20:39:03.43	+42:25:53.00	−215, +225	< .15	< .15	< .15	< .15
21413+5442		21:43:01.36	+54:56:16.28	−272, +168	< .18	< .18	*E*	*E*
22543+6145	CepA	22:56:19.14	+62:01:57.37	−220, +220	< .22	< .22	< .22	< .22
23116+6111	NGC 7538	23:13:45.62	+61:28:17:71	−279, +161	*A*?	*A*?	*A*	*A*

[a] E = Emission (see details in Table 2); A = Absorption (see details in Table 3); 3σ upper limits. (*) Observed only with the old autocorrelator.

Southern hemispheres (Baudry et al. 1997; Caswell & Vaile 1995) and the fact that the $J = \frac{5}{2}$ state lies immediately below $J = \frac{7}{2}$ suggest that $J = \frac{7}{2}$ maser emission could be frequently observed. We have used the most intense 5 cm OH emitters in our discrete source survey of 5 cm lines of OH (Baudry et al. 1997) to guide our search for new $J = \frac{7}{2}$ OH sources. Our 5 cm OH survey included nearly all of the major star-forming regions of the Northern hemisphere with bright H_2O masers and infrared flux densities brighter than 1000 Jy at 60 and 100 μm. In this work we have limited our selection of sources to 6035 MHz OH sources brighter than 0.5 Jy. Somewhat arbitrarily, we have added to this list three other strong 6035 MHz sources, G0.66−0.03 (in the SgrB2 complex), G11.90−0.14 and G20.23+0.07, which were first detected by Caswell & Vaile (1995), and three sources in the W33 region exhibiting strong 18 cm OH emission. Our final source list and J2000 coordinates are given in Table 1.

Observations of the two hyperfine transitions $F = 4 - 4$ (13 441.417 MHz) and $F = 3 - 3$ (13 434.637 MHz) of the $J = \frac{7}{2}$ state were performed with the Effelsberg 100-m telescope in May 5, 6 and 10, 1999. We used the cooled dual-channel 13 GHz system to simultaneously observe right and left circular polarizations (hereafter *RCP* and *LCP*). The on-source system temperatures were in the range 50 to 70 K depending on the source elevation. The pointing was checked by observing W3(OH) and other continuum sources. The telescope main beam was quite symmetrical and the full half-power beamwidth was measured to be 60 to 62 arcsec. The 13.44 GHz flux density scale was referred to observations of NGC 7027 and 3C 123 assuming average flux densities of 5.85 and 5.60 Jy respectively (see Ott et al. 1994). As for our 6030 and 6035 MHz OH spectra (Baudry et al. 1997) the 13.4 GHz *RCP* and *LCP* spectra were calibrated in terms of single polarization flux densities. However, the 3σ limits given in Table 1

Table 2. Gauss-fit line parameters of maser emission sources.

Source	13 441 MHz							
	Line id Number	Velocity ($km\,s^{-1}$)	Peak flux density (Jy)	Linewidth ($km\,s^{-1}$)	Line id Number	Velocity ($km\,s^{-1}$)	Peak flux density (Jy)	Linewidth ($km\,s^{-1}$)
W3(OH)								
	Right 1	−43.91	0.72	0.39	Left 4	−44.01	0.83	0.47
	2	−43.03	19.7	0.37	5	−43.11	25.6	0.30
	3	−42.37	7.72	0.35	6	−42.49	10.2	0.31
20081+3122								
(ON 1)	Right 1	−0.13	0.48	0.23	Left 3	−0.13	0.47	0.22
	2	+14.01	0.09	0.15	4	+14.02	0.08	0.19
21413+5442								
	Right 1	−61.47	0.39	0.16	Left 2	−61.47	0.38	0.17
G11.90−0.14								
	Right 1	+43.09	0.21	0.23				

are in terms of two polarization flux densities. All spectra were acquired in the position-switching mode and exhibited flat baselines and no radio interferences. The separation between spectral channels was 0.11 km s^{-1}. The W3(OH) $J = \frac{7}{2}$ maser emission was regularly observed for overall system check-up.

2.2. Results

A summary of the $F = 4 - 4$ and $F = 3 - 3$ observations is given in the last 4 columns of Table 1; *A* and *E* correspond to detection of absorption and emission features and *A*? indicates uncertain absorption. The upper limits are the unpolarized 3σ limits measured in our spectra; they lie in the range 0.1−0.2 Jy except for G0.66−0.03 where the limits are higher. In W3(OH), the ratio of 13 441 MHz ($J = 7/2$) to 6035 MHz ($J = 5/2$) peak flux densities is typically 1/5, and if our other targets were similar, then 13 441 MHz emission might be within our 3σ detection threshold. Three new but weak $J = \frac{7}{2}, F = 4 - 4$ maser emission sources have been discovered in this work in addition to W3(OH) (Table 2). Depending on the continuum flux density spectrum and strength of the observed compact HII regions, absorption features may be present and in fact have been observed in 7 sources (including W3(OH) where both broad absorption and narrow emission are present).

In Table 2 we give the emission line parameters (peak flux densities and linewidths at half peak intensity) for W3(OH) and the three new sources. These sources are masing because their linewidths are very narrow and because they are polarized in contrast with thermal emission sources. The line parameters are derived from a Gaussian analysis of the emission line profiles although the maser profiles may of course not be Gaussian-like.

The 13 441 MHz line profiles of the newly detected maser sources and of W3(OH) are shown in Fig. 1.

Absorption features are all weak and after examination of individual spectra we have added the *RCP* and *LCP* line profiles and degraded the spectral resolution to about 0.9 km s^{-1}. This allows us to reach signal to noise ratios higher than 3 to 4 for the weak 13 435 MHz line and over 10 in some sources at 13 441 MHz. Gauss fits to the smoothed profiles give us the LSR velocities, linewidths and peak intensities listed in Table 3. However, the linewidths are slightly uncertain because of the line smoothing procedure used here. In W3(OH) the 13 441 MHz absorption is noted with a question mark because of possible contamination by the strong maser emission (see Fig. 2 in Baudry et al. 1981).

In Table 4 we sum the *RCP* and *LCP* integrated flux densities to derive an estimate of the apparent maser luminosities in Jy km s^{-1} kpc^2 assuming the distance is known. In the case of 20081+3122 (ON1) we do not distinguish between the near and far kinematic distances. We performed similar calculations for the 5 cm OH lines (Baudry et al. 1997).

3. Individual sources and discussion

3.1. New $J = \frac{7}{2}$, $F = 4 - 4$ maser sources

We have discovered three new $J = \frac{7}{2}, F = 4 - 4$ maser sources in the direction of ON1, 21413+5442 and G11.90−0.14, in addition to W3(OH) which was detected for the first time more than 30 years ago (Turner et al. 1970). Previous $J = \frac{7}{2}$ observations were performed in a limited number of HII regions. Guilloteau et al. (1984) and Matthews et al. (1986) detected absorption features only. On the other hand, the tentative emission features reported by Balister et al. (1976) in M17 and W33 were not confirmed by Guilloteau et al. and by us in this work. Balister et al. reported a possible 3.7 Jy emission in G309.9+0.48 but give no detail apart from their spectrum; their detection looks rather convincing but was not repeated as far as we are aware. We thus have a total of 4 (and perhaps 5 with G309.9+0.48) $J = \frac{7}{2}, F = 4 - 4$ maser sources, in contrast with the nearly 100 sources detected in the 6035 MHz transition of OH from the Northern and Southern hemispheres. Therefore, the 13 441 MHz maser phenomenon is rare and W3(OH) remains exceptionally strong but not unique, as we have detected new sources.

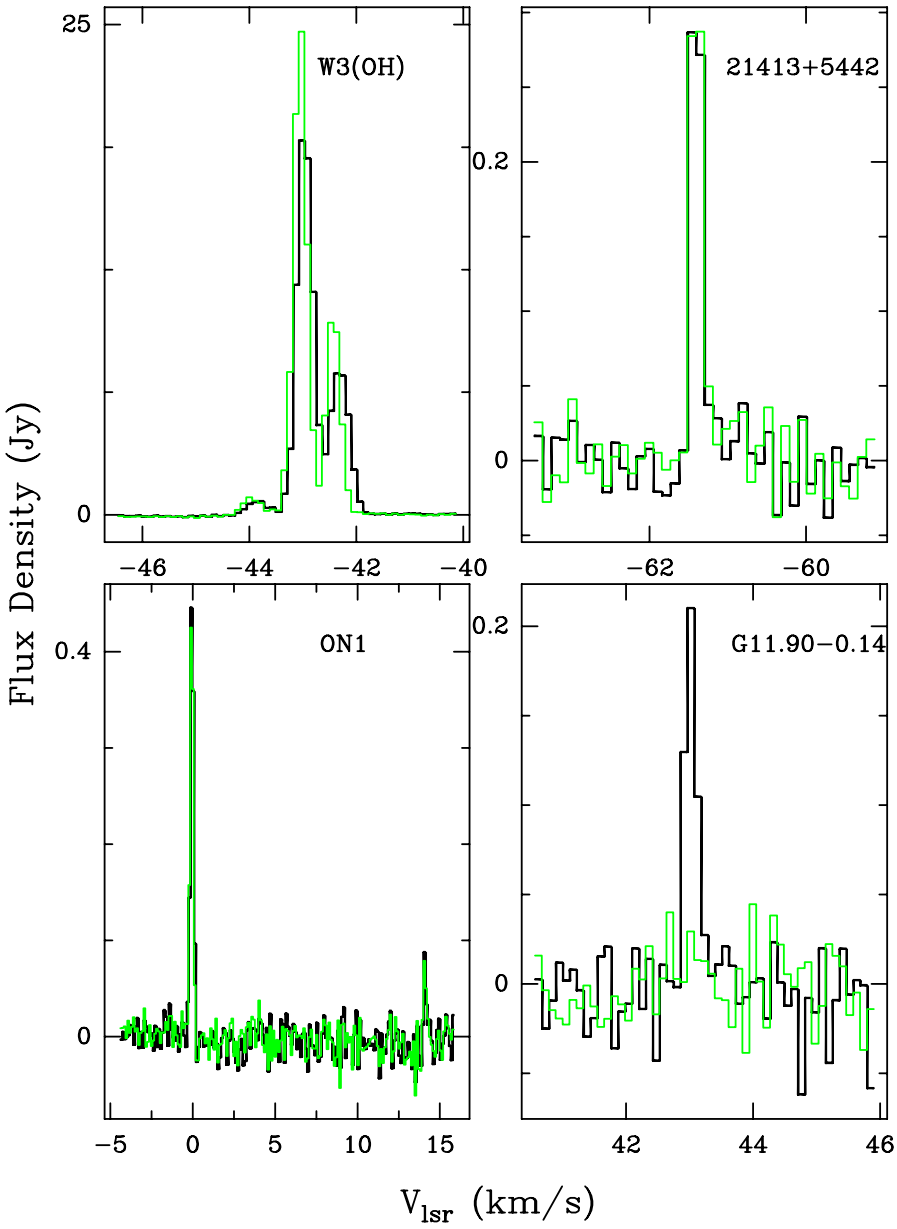

Fig. 1. $^2\Pi_{\frac{3}{2}}$, $J = \frac{7}{2}$, $F = 4-4$ spectra observed at 13 441 MHz in 1999 May with 0.1 km s^{-1} resolution. The line intensities are in Jy for a single polarization. The thicker and thinner lines are for right and left circular polarizations, respectively.

The 13 441 MHz peak flux densities are in the range 0.5 to 0.2 Jy in ON1, 21413+5442 and G11.90−0.14, and thus 50 to more than 100 times weaker than in W3(OH). Much weaker "intrinsic" luminosity in the new sources than in W3(OH) is also indicated by our results in Table 4. The observed linewidths, 0.15 to 0.25 km s^{-1} in the new sources and about 0.35 to 0.5 km s^{-1} in W3(OH), are similar to those observed at 6035/6031 MHz by Baudry et al. (1997). The intrinsic linewidths, 0.1 to 0.45 km s^{-1}, are thus less than the typical thermal linewidth of order 0.5 km s^{-1} in 100 K OH gas. This is expected in maser sources where the "initial" thermal linewidth may be significantly narrowed in spite of line re-broadening processes.

$J = \frac{7}{2}$ emission associated with the isolated ultra-compact HII region ON1 (IRAS 20081+3122 or G69.54−0.98; see e.g. Turner & Matthews (1984) for ionized shell structure) is most interesting because it has the strongest flux density after W3(OH). In addition, it exhibits two distinct velocity ranges separated by about 14 km s^{-1} suggesting complex kinematics. In the 13 441 MHz transition the low velocity feature is much stronger than the high velocity feature whereas the opposite is observed at 6035 MHz (Baudry et al. 1997), and in the ground-state with features around 11 to 16 km s^{-1} and 1 to 4 km s^{-1} (Argon et al. 2000). It is interesting to note that the relative OH positions measured by Argon et al. show that the 1665 MHz low velocity spots lie in a region well separated (by nearly

Table 3. Gauss-fit line parameters of absorption sources.

Source	Line	LSR Velocity ($km\,s^{-1}$)	Linewidth ($km\,s^{-1}$)	Peak flux density (Jy)
02219+6152				
W3(OH)	13 441	−45.25	3.14?	−0.26?
	13 435	−45.22	1.78	−0.18
W33C				
	13 441	+34.71	2.98	−0.06
	13 435	+34.80	4.88	−0.06?
W49				
	13 441	+03.98	4.22	−0.09
	13 435	+03.23	2.70	−0.22?
19111+1048				
	13 441	+55.67	4.65	−0.08
	13 435	+56.10	4.83	−0.04
W51				
	13 441	+63.33	1.80	−0.05
	13 435	+64.20	1.81	?
K3-50				
	13 441	−25.12	4.88	−0.08
	13 435	−24.71	2.39	−0.06?
NGC 7538				
	13 441	−59.67	5.24	−0.02

1 arcsec) from the 1665 and 1667 MHz high velocity spots. The OH gas kinematics against the compact HII region is thus complex and perhaps as complex as in the W3(OH) case. In the $J = \frac{5}{2}$ state, our 6035 MHz VLBI observations of the stronger 14-15 km s^{-1} features showed that the emission is distributed over an area comparable to that of the associated compact HII region (Desmurs & Baudry 1998) and to the ground-state OH area mapped by Argon et al. Both the low and high velocity features exhibit time variability at 6035 MHz. However, we have no VLBI maps of the lower velocity features and cannot conclude on their spatial distribution (although we have now completed both ground- and excited-state VLBI observations of ON1 with the EVN and the VLBA). Of course the spatial extent at 13 441 MHz could be much different from that in the lower J levels as we observed in W3(OH) (Baudry & Diamond 1998).

In both 21413+5442 and G11.90−0.14 the 13 441 MHz emission velocity is very close to the 6035 MHz emission velocity, and in G11.90−0.14 (see Caswell & Vaile 1995) the 6035 MHz source is essentially coincident with the ground-state 1665 MHz source.

3.2. Magnetic field strength

The 13 441 MHz right and left circularly polarized data can be used to estimate the magnetic field strength of identified Zeeman pairs. In the $^2\Pi_{\frac{3}{2}}, J = \frac{7}{2}, F = 4-4$ transition the velocity separation Δv between LCP and RCP Zeeman components is related to the magnetic field strength H by $\Delta v(\mathrm{km\ s^{-1}}) \approx 0.018\, H(\mathrm{mG})$.

In G11.90−0.14 there is no detected LCP feature; at the 6035 MHz transition near velocity +43 km s^{-1}, RCP likewise dominates (stronger than LCP by a factor of more than 2). In the sources ON1 and 21413+5442, both RCP and LCP features are observed (see Fig. 1) but, with the velocity resolution used here (about 0.11 km s^{-1}) there is no measurable separation between RCP and LCP. The average magnetic field is thus weaker than about 6 mG. In ON1 this result is consistent with our 6035 MHz VLBI observations which gave a field of −4 to −6 mG from four identified pairs (Desmurs & Baudry 1998). In W3(OH) the present work shows a consistent +0.1 $km\,s^{-1}$ velocity difference between the three main RCP and LCP velocity features. However, only VLBI observations can firmly identify spatially coincident Zeeman pairs. This was accomplished in W3(OH) by Baudry & Diamond (1998) who derived magnetic field strengths varying from 5 to 11 mG across a very small region against the compact HII region; they also found a relationship of the magnetic field gradient with the velocity field along the OH arc-like structure mapped by them. The latter observation and simple energetic considerations (see also Desmurs & Baudry 1998) suggest that the magnetic pressure tends to play a role in the dynamics of the OH dense gas.

3.3. Peculiar $J = \frac{7}{2}$, $F = 4-4$ and $F = 3-3$ maser emission and pumping models

Our source selection is biased toward intense $J = \frac{5}{2}$, 6035 MHz OH sources and it is only in the brightest 6035 MHz sources (see Table 3 of Baudry et al. 1997 for intrinsic $J = \frac{5}{2}$ luminosities) that we have found 13 441 MHz masers. However, not every bright 6035 MHz OH maser was detected at 13 441 MHz. This is the case for example of 18403−0417 or 19111+1048 which were much brighter at 6035 MHz than 21413+5442 and nearly as bright as ON1 in 1995 and 1994. Although only a few 13 441 MHz maser sources are known to date it seems that there is no strong relationship between the $J = \frac{5}{2}$ and $J = \frac{7}{2}$ maser emissions. This suggests that collisions and/or infrared pumping mechanisms which would correlate population inversions in the $J = \frac{5}{2}$ and $J = \frac{7}{2}$ states are not efficient. In addition, despite the especially small energy separation between the energy levels of the upper half of the $J = \frac{7}{2}$, Λ−doublet, it seems that in this high rotational state line overlap effects in infrared transitions do not play an important role in transferring the molecular populations between hyperfine levels because no strong $F = 3 - 3$ emission is observed.

No $J = \frac{7}{2}, F = 3 - 3$ emission was detected in the new sources or in any other sources (see Table 1). However, in W3(OH), we detect a weak $F = 3-3$ emission feature of about 70 mJy peak flux density lying around −42.4 km s^{-1} on the red wing of the main absorption feature. It is more than two orders of magnitude weaker than the $F = 4 - 4$ transition at the same velocity. This feature is narrow (2 to 3 channels) and polarized (only LCP emission is detected in our spectra) and thus suggests weak maser emission. Emission at the same velocity is

Table 4. Integrated flux densities of maser sources at 13 441 MHz.

Source	l, b	$\int S\mathrm{d}v$ (Jy km s^{-1})		Distance (kpc)	Luminosity (Jy km s^{-1} kpc^2)
		Right	Left		
W3(OH)	133.94+1.06	10.40	11.27	2.2	104.88
20081+3122	69.54−0.98	0.12	0.12	1.0,5.0	0.22, 5.5
21413+5442	98.04+1.45	0.06	0.06	7.5	6.75
G11.90−0.14	11.90−0.14	0.05		5.1	1.3

also present in the $F = 3 - 3$ spectrum of Güsten et al. (1994) (see their Fig. 2).

The lack of apparent correlation between the $J = \frac{5}{2}$ and $J = \frac{7}{2}$ emission line intensities may be due in part to non simultaneous variability of the 13 441 and 6035 MHz masers. Variability was well demonstrated in all three main features observed at 13 441 MHz in W3(OH) (see Baudry & Diamond 1998), and our observations of 1999 May (this work) show that these features still vary. The −43.1 km s^{-1} to −42.4 km s^{-1} relative flux density ratio is around 2.5 to 2.7 in 1999 whereas the same ratio was about 1.8 in our VLBA spectra of 1995 September.

The OH excitation models of Pavlakis & Kylafis (1996a and b, 2000) explain theoretically several characteristics of the maser lines of OH at 18, 6 and 5 cm. As suggested by Pavlakis and Kylafis, their calculations are in agreement with the low J OH observations because the collision rate coeficients are better known in the lower rotational states. This idea is strengthened by the the recent OH model results of Cragg et al. (2002). However, the Cragg et al. results differ significantly from those of Pavlakis and Kylafis for the $J = \frac{5}{2}$ transitions at 6 GHz because more energy levels (and new collision rates) have been included in their calculations. This new model is potentially useful to predict the behaviour of the OH lines in the high energy $J = \frac{7}{2}$ state. On the other hand, the earlier predictions of Gray et al. (1991, 1992) remain uncertain for the $J = \frac{7}{2}$ lines not only because of the collisional rate deficiency mentioned above, but also because they predict maser emission of the 13 435 MHz transition whereas only one weak 13 435 MHz emission source was observed in this work. The model results of Cesaroni & Walmsley (1991) and Cesaroni (2002) show that all 13.4 GHz lines do not easily mase. However, under special physical conditions (e.g. dust temperature greater than the gas temperature or dominant external IR field) the relevant $J = \frac{7}{2}$ levels may be weakly inverted and at the same time strong $J = \frac{5}{2}$ masers are obtained in the 6 GHz lines. This is in agreement with our observations.

Our results clearly demonstrate that the 13 441 MHz OH masers are difficult to excite. This is reflected in the low number of new $J = \frac{7}{2}$ maser emission sources detected in this work and in $F = 4 - 4$ luminosities (Table 4) always much weaker than at 6035 MHz. In addition, the overall velocity extent is always small (2.5 km s^{-1} in W3(OH) at 13 441 MHz compared to about 8 and 10 km s^{-1} at 5 and 18 cm). ON1 is an exception with two groups of features separated by about 14 km s^{-1} at 13 441 MHz, but each group has narrow velocity extent. This velocity separation is similar to that observed at 5 and 18 cm (Baudry et al. 1997; Argon et al. 2000). The 18 cm OH spots are distributed across the HII region (Argon et al. 2000), while our knowledge of the relative 13 441 and 6035 MHz spatial location await analysis of our VLBI results. In any case the peak flux densities and luminosity are markedly weaker in the $J = \frac{7}{2}$ rotational state.

Cesaroni (2002) made an interesting new suggestion concerning the narrow velocity spread of the 13 441 MHz maser. He has noted that some of the far infrared transitions $^2\Pi_{\frac{1}{2}}, J = \frac{5}{2} \rightarrow {}^2\Pi_{\frac{3}{2}}, J = \frac{7}{2}$ and $^2\Pi_{\frac{3}{2}}, J = \frac{7}{2} \rightarrow {}^2\Pi_{\frac{3}{2}}, J = \frac{5}{2}$ are separated by about 2 to 2.5 km s^{-1} which is just the maximum velocity spread observed in the 13 441 MHz maser emission. It is possible that non-local overlap effects due to velocity fields greater than about 2 km s^{-1} in the OH gas might enhance the optical depth of these far infrared lines thus resulting in easier thermalisation and easier quenching of the $J = \frac{7}{2}$ maser. It would be useful to quantitatively test whether non-local overlap effects play a role in the narrow velocity maser emission at 13 441 MHz.

We conclude from our observations that infrared and collisional pumpings are less efficient in higher energy levels, a general trend predicted by the model work of Cesaroni & Walmsley (1991). This is especially true in the $J = \frac{7}{2}$ state for which, in contrast with all other energy levels exhibiting maser emission, there is *no direct connection* with the OH ground-state levels. This fact could explain the observed small velocity extent (see also suggestion above) and why the 13 441 MHz emission mapped in W3(OH) by Baudry and Diamond is confined to a very compact area against the HII region. (We further suggested that this area marks the site of the embedded O-type star that powers the HII region.)

3.4. Absorption sources

Table 3 shows that absorption by the $F = 4 - 4$ transition is always weak except in W3(OH) and that the $F = 3 - 3$ main line transition is even weaker or not detectable. The observed $F = 4 - 4$ to $F = 3 - 3$ intensity ratio lies in the range 1 to 2 whereas the LTE relative line strength is $\left(\frac{F=4-4}{F=3-3}\right) = \left(\frac{35}{27}\right) \approx 1.3$. It is difficult however to draw any firm conclusion from this as the signal is weak and as we do not know what fraction of the OH cloud covers the HII region. Gas clumpiness is in fact well observed in W3(OH) in the low J levels as well as in the $^2\Pi_{\frac{3}{2}}, J = \frac{9}{2}$ high energy level (Baudry & Menten 1995). In addition, in at least two sources, W3(OH) and 1911+1048, our

high spectral resolution observations of the $J = \frac{7}{2}$ transitions clearly show asymmetric line profiles, a fact that can be interpreted by two or more overlapping spectral components. (The highly sensitive observations of Güsten et al. 1994, in W3(OH) demonstrate that there are two Gaussian velocity components in the $F = 3 - 3$ transition.)

In the optically thin case absorption features give a direct estimate of the opacity (from the line-to-continuum ratio), and hence of the ratio $\frac{N}{T_{\rm ex}}$ where N is the column density and $T_{\rm ex}$ the excitation temperature. In the strongest absorption sources we derive apparent $F = 4 - 4$ opacities of the order of 0.01 (W48 and K3−50) and ≈0.014 in 19111+1048. This is nearly 10 times less than for W3(OH). Our opacity measurements are in agreement with the earlier results of Guilloteau et al. (1984) and Matthews et al. (1986) obtained in several HII/OH regions. Combining absorption results from several J levels Guilloteau et al. estimated $\frac{N(\rm OH)}{T_{\rm ex}} \approx 1 - 5 \times 10^{14}$ cm^{-2}/K. Hence, we expect OH column densities of the order of a few 10^{16} cm^{-2} for OH excitation and rotational temperatures around 100 K, and over 10^{17} cm^{-2} in W3(OH).

4. Conclusions

Our observations can be summarized as follows:

1. The high energy $J = \frac{7}{2}$ levels of OH (290 K above the ground-state) are more difficult to excite than lower J rotational levels; this trend is expected from theory of OH excitation. However, three new but weak $J = \frac{7}{2}, F = 4 - 4$ maser sources were discovered at 13 441 MHz in a sample of 27 known $J = \frac{5}{2}, F = 3 - 3$ maser sources.

2. The new sources exhibit 13 441 MHz peak flux densities 50−100 times, or more, weaker than in W3(OH). W3(OH) remains exceptionally strong but is not unique in terms of $J = \frac{7}{2}$ maser emission.

3. The 13 441 MHz velocity extent is very small and does not exceed 2.5 km s^{-1} in the brightest source W3(OH). This is in contrast with observations of lower J rotational levels and could result from a combination of lower excitation of higher J levels and non-local line overlap effects of far infrared transitions involving the $J = \frac{7}{2}$ level.

4. $J = \frac{7}{2}$, 13 441 MHz maser emission from the ultracompact HII region ON1 is spectrally narrow but is observed in two distinct groups of features, as in the $J = \frac{5}{2}$ and $J = \frac{3}{2}$ states. This suggests complex dynamics of the OH gas surrounding the young HII region.

5. We have not detected any strong $J = \frac{7}{2}, F = 3 - 3$ emission at 13 435 MHz. In W3(OH), however, we have observed a weak, narrow and polarized emission around −42.4 km s^{-1} on the red wing of the main absorption feature.

6. $J = \frac{7}{2}$, 13 441 and sometimes 13 435 MHz OH weak absorptions were observed in 7 compact HII regions. The apparent OH opacities are of the order of 0.01 in general, and consistent with total OH column densities of a few 10^{16} cm^{-2} for OH rotational temperatures around 100 K.

Acknowledgements. The authors would like to thank the referee, Dr. J. Caswell, for useful comments, and Dr. R. Cesaroni for his suggestion concerning line overlap effects in high energy levels of OH. We also wish to thank the Effelsberg staff for their help during the observations.

References

Argon, A. L., Reid, M. J., & Menten, K. 2000, ApJS, 129, 159
Balister, M., Gardner, F. F., Knowles, S. H., Whiteoak, J. B. 1976, Proc. Astron. Soc. Austr., 3, 59
Baudry, A., & Diamond, P. J. 1998, A&A, 331, 697
Baudry, A., Desmurs, J. F., Wilson, T. L., & Cohen, R. J. 1997, A&A, 325, 255
Baudry, A., & Menten, K. M. 1995, A&A, 298, 905
Baudry, A., Walmsley, C. M., Winnberg, A., & Wilson, T. L. 1981, A&A, 102, 287
Caswell, J. L., & Vaile, R. A. 1995, MNRAS, 273, 328
Cesaroni, R., & Walmsley, C. M. 1991, A&A, 241, 537
Cesaroni, R. 2002, private communication
Cragg, D. M., Sobolev, A. M., & Godfrey, P. D. 2002, MNRAS, 331, 521
Desmurs, J. F., & Baudry, A. 1998, A&A, 340, 521
Desmurs, J. F., Baudry, A., Wilson, T. L., Cohen, R. J., & Tofani, G. 1998, A&A, 334, 1085
Gray, M. D., Doel, R. C., & Field, D. 1991, MNRAS, 252, 30
Gray, M. D., Field, D., & Doel, R. C. 1992, A&A, 262, 555
Guilloteau, S., Baudry, A., Walmsley, C. M., et al. 1984, A&A, 131, 45
Güsten, R., Fiebig, D., & Uchida, K. I. 1994, A&A, 286, L51
Matthews, H. E., Baudry, A., Guilloteau, S., & Winnberg, A. 1986, A&A, 163, 177
Ott, M., Witzel, A., & Quirrenbach, A., et al. 1994, A&A, 284, 331
Pavlakis, K. G., & Kylafis, N. D. 1996a, ApJ, 467, 300
Pavlakis, K. G., & Kylafis, N. D. 1996b, ApJ, 467, 309
Pavlakis, K. G., & Kylafis, N. D. 2000, ApJ, 534, 770
Turner, B. E., & Matthews, H. E. 1984, ApJ, 277, 164
Turner, B. E., Palmer, P., & Zuckerman, B. 1970, ApJ, 160, L125